J MATER SCI 41 (2006) 3631–3644

Microstructure and mechanical properties of rheo-diecast AZ91D magnesium alloy

Z. FAN*, G. LIU, Y. WANG
BCAST (Brunel Centre for Advanced Solidification Technology), Brunel University, Uxbridge, Middlesex, UB8 3PH, UK
E-mail: Zhongyun.Fan@brunel.ac.uk

Published online: 21 April 2006

A new semisolid metal processing technology, rheo-diecasting (RDC) has been developed for production of Mg-alloy components with high integrity. The RDC process innovatively combines the dispersive mixing power of the twin-screw mechanism for creation of high quality semisolid slurry and the high efficiency, low cost nature of the high pressure die casting (HPDC) process for component shaping. AZ91D Mg-alloy was used to optimise the RDC process and to establish its advantages over both the HPDC process and other existing semisolid processing techniques. In this paper we present the RDC process for processing Mg-alloys and the resulting microstructure and mechanical properties of RDC AZ91D alloy. The solidification behaviour of the Mg-alloys in the RDC process and the co-relationships between microstructure and mechanical properties of the RDC AZ91D alloy are discussed. It was found that the RDC process is capable of producing Mg-alloy samples with close-to-zero porosity and a fine, uniform microstructure throughout the entire sample irrespective of the section thickness. Compared with those obtained by other existing processing techniques, the RDC samples have substantially improved or equivalent mechanical properties, with the tensile elongation showing more than 100% improvement.

1. Introduction

Due to increasing environmental concerns and tightening government regulations on CO_2 emissions, reducing vehicle weight and improving fuel economy are becoming increasingly important in the automobile industry. For instance, the European and North American car producers are committed to reducing fuel consumption by 25% and thereby achieving 30% reduction in CO_2 emission by the year 2010 [1]. Magnesium alloys, as the lightest structural materials, are very suitable for applications in the automotive industry to assist the realisation of such goals. In the past few years we have seen a 15% average annual increase of Mg usage in the automobile industry, and it is predicted that this growth trend will continue well into the first decade of the 21st century and beyond. Although the automobile industry will continue to be the dominant driving force for the future growth in magnesium application, other areas, such as aerospace, electronics and health care, will take a substantial share of the magnesium market in the near future.

Currently, nearly all the current applications of Mg-alloys are achieved by high pressure die-casting (HPDC) and are limited to a few casting alloys, such as AZ91D and AM60. The HPDC process is characterised by high efficiency, high production volume and low production cost. However, the HPDC components contain a substantial amount of porosity due to gas entrapment during die filling and hot tearing during the solidification in the die cavity [2]. Such porosity not only deteriorates mechanical properties and limits the applications to non-stress or low-stress components, but also denies the opportunity for property enhancement by subsequent heat treatment. Further growth in Mg applications will largely depend on the successful development of new processing technologies capable of producing high quality, low cost components and new alloys with higher operating temperatures [3].

One of the promising technologies capable of producing high integrity components is semisolid metal (SSM) processing [4, 5]. In conventional die casting, liquid metal is usually forced into a mould cavity at such a high speed that the flow becomes turbulent or even atomised, leading to high porosity in the final components. In contrast, SSM processing uses a SSM slurry with substantially increased viscosity, resulting in a controlled die filling and

*Author to whom all correspondence should be addressed.
0022-2461
DOI: 10.1007/s10853-006-6248-x

close to zero porosity in the final components. Compared with conventional die casting, SSM processing has a number of advantages, such as low porosity, heat treatability, consistency and soundness of mechanical properties, the ability to make complex component shapes and longer die life [4, 5].

One of the most popular SSM processes used currently is thixoforming [6], in which non-dendritic alloys pre-processed by electromagnetic stirring [7] are reheated to the semisolid region prior to the component being shaped by either casting (thixocasting) or forging (thixoforging). It is therefore a two-stage process. The high cost of pre-processed non-dendritic raw materials is by far the greatest obstacle to the development of the full potential of this approach [8]. In addition, polymer injection moulding techniques have also been introduced into the SSM processing field. One such process is thixomoulding [9], which was developed by Dow Chemicals and currently marketed by Thixomat. Due to the lack of reliable and quality feedstock supply, thixoforming of Mg-alloys has been very scarce. So far, only thixomoulding of thin-walled components has achieved some success with electronic housing applications. To overcome the technical and economical difficulties faced by the thixo-processing route, the rheo-route of SSM processing has become popular for research and development in recent years [10]. This includes the new rheocasting (NRC) process developed by UBE [11], the SSR^{TM} process developed by MIT [12] and the continuous rheoconversion process (CRP) developed by WPI [13]. A common feature of rheo-processing techniques is that they all use molten alloy as a starting material, therefore eliminating the need for specially prepared feedstock materials. Although the rheo-processing techniques are still in the development stage, they appear to be promising for future industrial applications.

AZ91D alloy is the most widely used cast Mg-alloy. It contains around 9 wt.% Al, less than 1 wt.% Zn and other minor alloying elements such as Mn, Si and Be. Al increases fluidity and therefore increases castability, but decreases creep resistance due to the formation of the $Mg_{17}Al_{12}$ β-phase; Zn addition assists strengthening but increases the susceptibility to hot tearing. The composition of AZ91D maintains a good balance between castability and reasonable combination of mechanical strength and ductility in the as-cast condition. In addition, AZ91D alloy is heat treatable due to the precipitation of the β-phase from the supersaturated α-Mg solid solution.

In this paper we report a new semisolid processing technique, the rheo-diecasting (RDC) process. The microstructure and mechanical properties of RDC AZ91D Mg-alloy will be presented and compared with those produced by other processes. The discussion will be focused on solidification behaviour of the AZ91D alloy under the RDC conditions and the co-relationships between processing, microstructure and mechanical properties of RDC AZ91D alloy.

2. The RDC process for Mg-alloys

The RDC process is an innovative one-step SSM processing technique for manufacturing near-net shape components of high integrity, directly from liquid Mg-alloys. The process innovatively adapts the well-established high shear dispersive mixing action of the twin-screw mechanism, to the task of *in situ* creation of SSM slurry with fine and spherical solid particles, followed by direct shaping of the SSM slurry into a near-net shape component using the existing cold chamber HPDC process.

Figs 1a and b schematically illustrate the rheo-diecasting process for manufacturing Mg-alloy components of different sizes. It consists of two basic functional units, a slurry supply system and a standard cold chamber HPDC machine. For small components (less than 3 kg shot weight), the slurry supply system only has a twin-screw slurry maker (Fig. 1a); while for large components (more than 3 kg shot weight) the slurry supply system consists of a twin-screw slurry maker and a slurry accumulator (Fig. 1b). The twin-screw slurry maker has a pair of screws rotating inside a barrel. The screws have specially designed profiles to achieve co-rotation, full intermeshing and self-wiping. The fluid flow inside the slurry maker is characterised by high shear rate and high intensity of turbulence. The basic function of the twin-screw slurry maker is to convert the liquid alloy into high quality semisolid slurry through solidification of the liquid alloys under high shear rate and high intensity of turbulence. It works in a batch manner, providing slurry every 20–30 s. During the slurry making process, there is an enormous amount of ever-changing interfacial area between the solidifying alloy and the screws and the barrel. This makes the slurry creating process extremely efficient for heat extraction. The slurry accumulator, as shown in Fig. 1b, is designed to deal with large components. For instance, a 12 kg shot will require a 3 kg slurry maker to operate 4 times in order to accumulate enough semisolid slurry for a single shot. A blade type stirrer is fitted in the accumulator to prevent particle agglomeration and to maintain the slurry uniformity. By utilising a slurry accumulator, the problem associated with decreasing efficiency with increasing the capacity of the twin-screw slurry maker, can be successfully solved. In the RDC process, a standard cold chamber HPDC machine is used to achieve the final component shaping. No modification to the HPDC machine is required. To avoid oxidation, a protective gas mixture of N_2 containing 0.4vol%SF6 was used in the melting furnace, the twin-screw slurry maker and the slurry accumulator.

During the rheo-diecasting process, a predetermined dose of liquid alloy from the melting furnace is fed into the slurry maker. The liquid alloy is rapidly cooled to the SSM processing temperature, while being mechanically sheared by a pair of closely intermeshing screws, converting the liquid into semisolid slurry. Setting the barrel at different temperatures controls the solid fraction of the

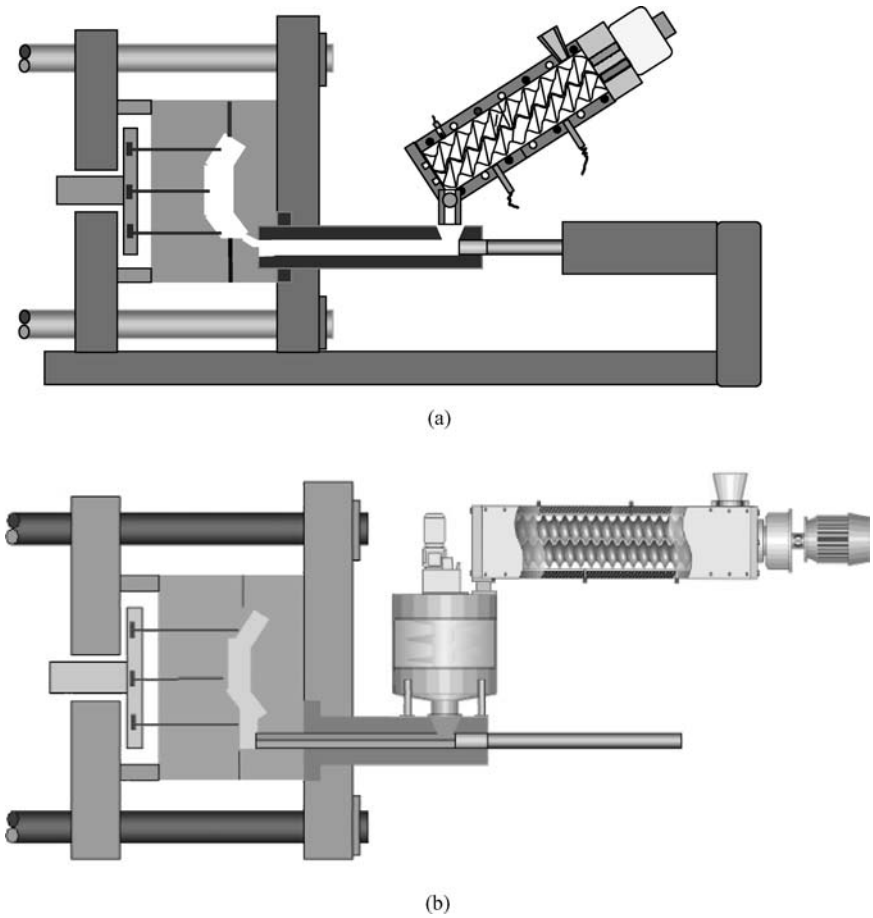

Figure 1 Schematic illustrations of the rheo-diecasting (RDC) process for shot weight (a) less than 3 kg and (b) more than 3 kg Mg-alloy.

semisolid slurry. The semisolid slurry is then transferred to a slurry accumulator. Once the shot weight is achieved in the accumulator, the semisolid slurry is transferred to the shot chamber of the HPDC machine for component shaping.

It is important to point out that, in the RDC process, the component shaping process (solidification of SSM slurry inside the die cavity and the preparation of the die for next shot) and the slurry making process are parallel, rather than sequential. Once the SSM slurry is transferred to the shot chamber of the HPDC machine, the slurry supply system starts to prepare slurry for the next shot. The slurry making process is more efficient than the component shaping process, and the cycle time of the RDC process is, therefore, dictated by the component shaping process. Consequently, the RDC process has a shorter cycle time than the conventional HPDC process, since a SSM slurry feed has less heat to be removed than a fully liquid feed.

3. Experimental procedures

The AZ91D alloy used in the present study was provided by MEL (Magnesium Elektron, Manchester, UK) and the actual composition is listed in Table I. The Mg alloy ingot received from MEL was melted at 675°C under the protection of a N_2 + 0.5 vol% SF_6 gas mixture and fed into the slurry maker at 650°C. The slurry maker was operated at a temperature, ranging from 585 to 600°C, corresponding to a desired solid volume fraction for the AZ91D alloy, and at a fixed rotation rate of 500 rpm, producing a shearing rate of 534 s^{-1}. The AZ91D alloy was sheared in the slurry maker for 35 s and then transferred into a 280-ton cold chamber HPDC machine (LK Machinery, Hong Kong), which was used for casting standard test samples. The die used for casting test samples has six cavities, of which four are tensile test samples and two are Charpy test samples. The dimensions of the tensile test samples are 6 mm in gauge diameter, 60 mm in gauge length and 150 mm in total length.

The resulting AZ91D Mg alloy samples, produced by both HPDC and RDC processes, were subjected to heat treatment. This was carried out according to the procedure and parameters optimised in a detailed study [14] and the

TABLE I Chemical composition (wt.%) of the AZ91D alloy ingot used in this work

Zn	Al	Si	Cu	Mn	Fe	Ni	Be	Others Each
0.67	8.8	0.03	< 0.001	0.22	0.002	0.0005	0.0011	< 0.01

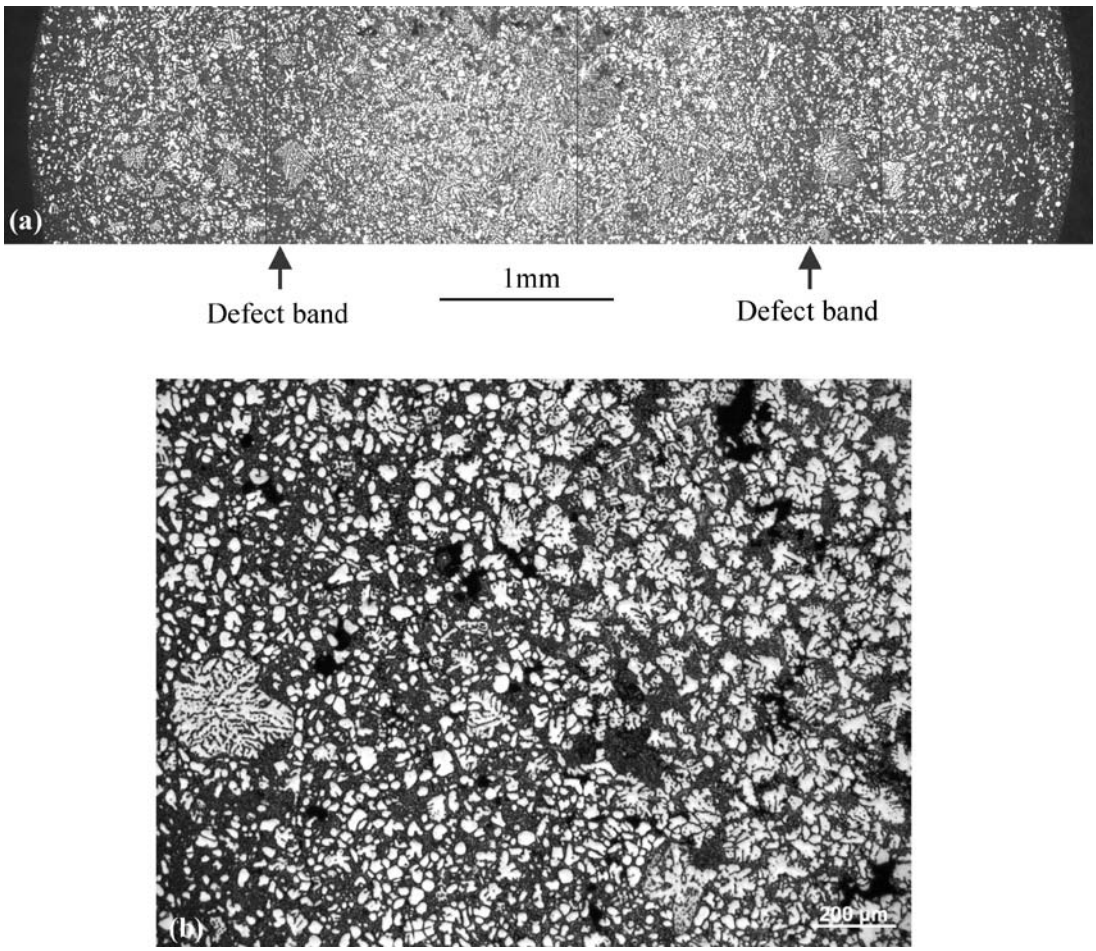

Figure 2 Optical micrographs showing, (a) the as-cast microstructure through the entire cross-section of a ϕ6 mm AZ91D alloy bar, and (b) the presence of large primary dendrites in the AZ91D alloy produced by the HPDC process.

recommendation by the ASM Speciality Handbook [15]. In the present study, solution treatment was carried out in air, with protection of carbon powder on the surface of the samples, at 413°C for 5 h (T4). The samples were then quenched in water before being aged at 216°C for 5.5 h (T6). A T5 treatment was also carried out at 216°C for 5 h for the AZ91D Mg-alloy.

The mechanical properties of the alloy in its as-cast and heat treated states were characterised with tensile tests carried out at room temperature with a Lloyd Instrument EZ50 tensile test machine, using the standard ϕ6 mm samples with 50 mm gauge length. The crosshead speed was 1 mm/min.

The microstructure of the alloy was examined by optical microscopy (OM) with quantitative metallography, scanning electron microscopy (SEM) and X-ray diffractometry (XRD). The specimens for OM and SEM were prepared by the standard technique of grinding with SiC abrasive paper and polishing with an Al_3O_2 suspension solution, followed by etching in an aqueous solution of 60 vol% ethylene glycol, 20 vol% acetic acid, 1 vol% concentrated HNO_3. A Zeiss optical microscope was utilised for the OM observations and the quantitative measurements, while a Jeol JXA-840A scanning electron microscope, equipped with an energy dispersive spectroscopy (EDS) facility, was used to perform the SEM examinations with an accelerating voltage of 20 kV. XRD analysis was carried out in order to identify the phases present in the alloys. A Philips 1700 X-ray diffractometer was used, with CuK_α radiation, operated at a voltage of 36 kV and an anode current of 26 mA.

4. Results

4.1. Microstructure of AZ91D alloy produced by conventional HPDC

Conventional HPDC was used to obtain benchmark results for AZ91D alloy. Fig. 2a represents the typical microstructure of HPDC AZ91D alloy through a cross section of a ϕ6 mm bar. There is a chill zone near the sample surface, which has a fine structure and is enriched with Al compared with the rest of the sample. This chill zone, sometimes referred as the surface layer in the literature, is believed to have a strong influence on the mechanical properties of die cast samples [16]. The porosity is concentrated in the centre of the sample and consisted of both entrapped gas bubbles and cracks caused by hot tearing. In addition, there is a dark circular region observed on the

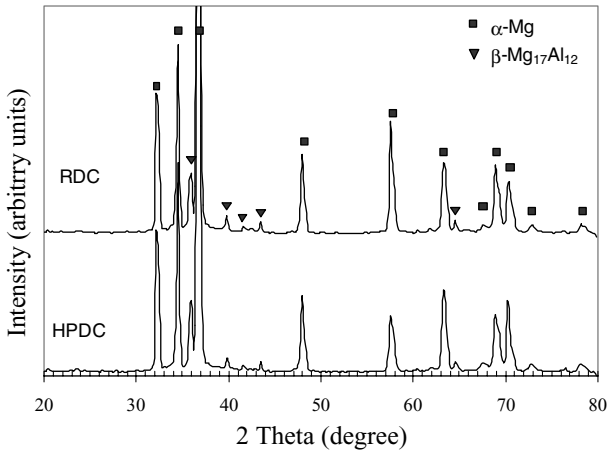

Figure 3 X-ray diffraction traces showing the phases present in the AZ91D alloy processed by both HPDC and RDC processes.

cross section as marked in Fig. 2a. Detailed microstructural analysis indicates that this region is concentred with hot cracks and enriched with the β-phase. This defect band is a typical feature of HPDC Mg-alloy castings, as has been investigated in detail by Bowles *et al*. [17].

In addition to the chemical segregation and defect formation in the HPDC sample, the formation of large dendritic primary α-phase is an important feature of HPDC AZ91D alloy, as shown in Fig. 2b with a higher magnification. It is believed that such dendritic particles are formed in the shot sleeve prior to mould filling. The high shear rate that the melt experienced at the gate (estimated to be as high as 10^5 s^{-1} by Sequeira *et al*. [16]), fragmented the dendrites resulting in the morphology of the primary phase observed in Fig. 2b. It is also evident from Fig. 2b that some of the dendrites formed in the shot sleeve had survived the high shear at the gate and were present in the final solidified microstructure.

4.2. Microstructure of RDC AZ91D alloy

In order to check the effects of melting and rheo-diecasting on the chemical composition of the AZ91D alloy, chemical analysis was carried out on samples taken from the melting furnace and the RDC sample. The results are presented in Table II and are compared with the chemical compositions of the AZ91D ingot. There was very little change in the content of the alloying elements. Perhaps more importantly, there was little change in Fe content after both melting and rheo-diecasting, with the Fe content in the RDC sample being well within the specification of AZ91D alloy.

The X-ray diffraction traces of AZ91D alloy produced by both RDC and HPDC processes are presented in Fig. 3. The results indicate that only the α-Mg phase and the β-$Mg_{17}Al_{12}$ phase were present in both samples. No evidence for the presence of any other phases was detected by the X-ray analysis.

One of the most important features of SSM processing is to achieve laminar die filling. To check this the die

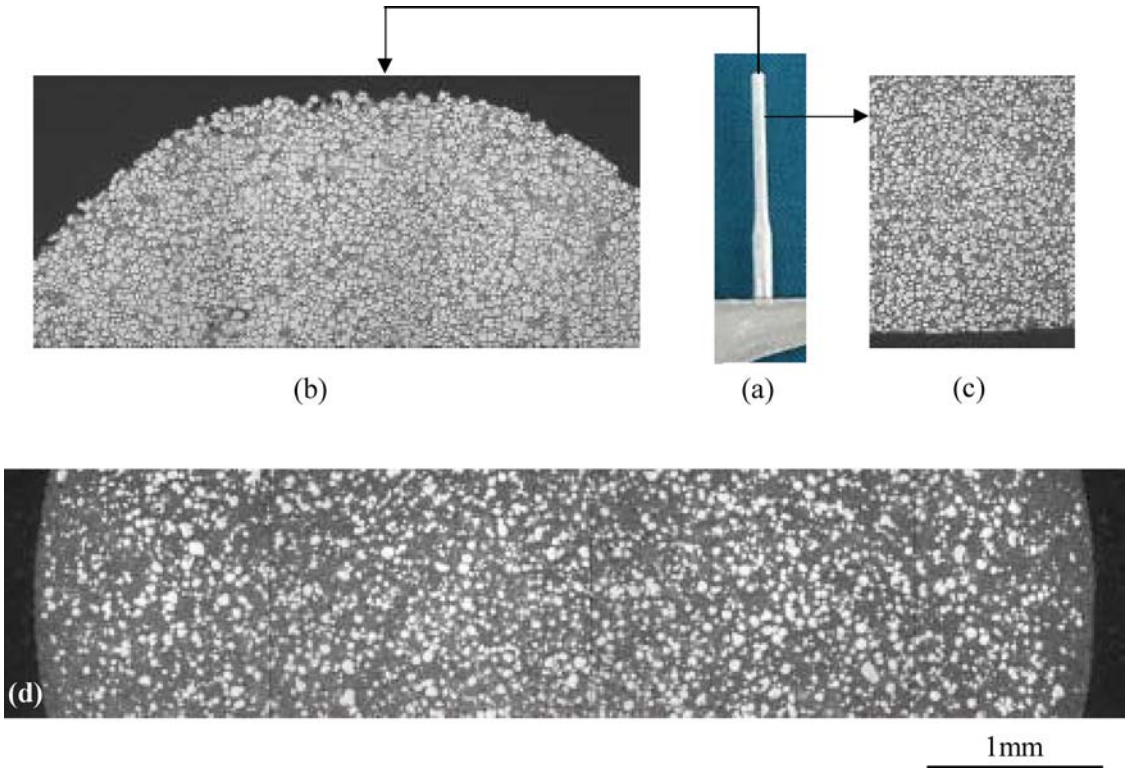

Figure 4 (a) Photograph of a half-filled test bar: (b) micrograph showing the laminar flow front during mould filling, (c) micrograph showing the surface condition produced by the RDC process, and (d) a montage of optical micrographs showing the as-cast microstructure throughout the entire cross-section of a ϕ6 mm AZ91D alloy bar produced by the RDC process.

TABLE II The actual chemical composition (wt.%) of AZ91D alloy at different processing stages

AZ91D	Zn	Al	Si	Cu	Mn	Fe	Ni	Be	Others Each
Ingot	0.67	8.76	0.047	0.024	0.28	0.0038	0.0015	0.0011	< 0.01
After melting	0.66	8.55	0.046	0.022	0.21	0.0039	0.0011	0.0008	< 0.01
After RDC	0.63	8.52	0.048	0.024	0.18	0.0040	0.0011	0.0007	< 0.01

cavity was deliberately filled half way so the conditions at the flow front could be examined. The photograph of the half filled sample and the microstructure at the flow front are presented in Fig. 4a–c, which shows that the flow front during the mould filling is parabolic and smooth, indicating that the mould filling was laminar under the optimised conditions. In addition, the sample surface was sharp and tidy (Fig. 4c), indicating a very good surface finish produced by the RDC process. It should be pointed out that the micrographs in Fig. 4a–c contain 30% large, primary solid particles, while the smaller α-Mg particles were formed inside the die through secondary solidification of the remaining liquid in the semisolid slurry. This will be discussed further in later sections.

Fig. 4d presents a montage of micrographs showing the as-cast microstructure through the entire cross-section of a 6 mm diameter AZ91D alloy bar, produced by the RDC process. In contrast to the microstructure of HPDC samples (Fig. 2a), the primary particles in the RDC samples were fine and spherical. There was no entrapped gas porosity, and only very fine hot cracks (a few microns in size) could be observed occasionally. The total porosity was much less than 0.5%. Quantitative metallography was used to quantify the distribution of the primary particles in the samples with different solid fractions. The results are presented in Fig. 5 which indicates that the primary solid phase had a uniform distribution throughout the entire cross section of the sample. Only a slightly lower solid fraction was observed at the sample surface, which coincides with a slight enrichment of Al in the surface region.

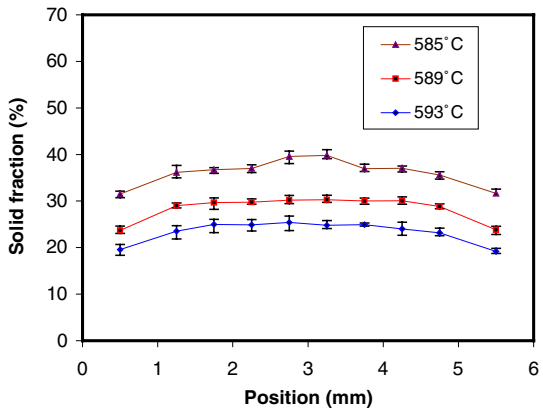

Figure 5 A graph to show the variation of volume fraction of the primary α-Mg particles through the cross section of 6 mm AZ91D alloy bars processed at different temperatures.

In the RDC process the variation of solid fraction is achieved by changing the barrel temperature. Fig. 6a shows the microstructure of AZ91D alloy processed at 600°C, which roughly coincides with its liquidus. The primary particles were fine in size and less spherical in morphology. It is likely that such primary particles were formed in the shot sleeve, and fragmented by the intensive shear flow at the gate. However, different from the non-uniform microstructure produced by HPDC process (Fig. 2b), the microstructure here was extremely uniform throughout the entire sample. This is referred to as liquidus rheocasting [18]. By reducing the processing temperature below the liquidus, semisolid slurries with different solid fractions could be produced. Fig. 6b–e show the microstructure of RDC AZ91D alloy processed at different temperatures. The quantified volume fraction, particle size and morphology are summarised in Table III. When the processing temperature decreased from 597°C to 585°C the solid fraction increased from 0.091 to 0.314. However, the particle size and morphology appeared to be fairly constant, with the particle size being around 40μm and the shape factor being around 0.78. This indicates that both particle size and morphology are independent of processing temperature. The measured solid fraction data are presented in Fig. 7 as a function of the processing temperature, where the equilibrium solid fractions in the liquid-solid region are also shown. Thermo-Calc and MG-DATA (a Mg-database developed by Thermo-Tech Ltd, Guildford, UK) were used to assess the thermodynamic properties of the AZ91D alloy and to theoretically predict the equilibrium solid fractions for the AZ91D alloy with a constant Zn content (0.67 wt.%). The experimental data is fairly close to the thermodynamic predictions, indicating the solidification inside the twin-screw slurry maker was close to equilibrium.

Solidification inside the twin-screw slurry maker under intensive forced convection is referred to as primary solidification. The solidification of the remaining liquid of the

TABLE III Summary of the quantitative metallography results of the RDC AZ91D samples produced at different temperatures (corresponding to Fig. 6)

Shearing temperature (°C)	Solid fraction (%)	Particle size (μm)	Shape factor
585	31.4 ± 1.17	42.6 ± 2.89	0.76 ± 0.02
589	25.1 ± 0.56	40.9 ± 2.80	0.75 ± 0.03
593	19.1 ± 0.25	39.7 ± 3.10	0.80 ± 0.03
597	9.1 ± 2.95	39.2 ± 0.91	0.78 ± 0.01

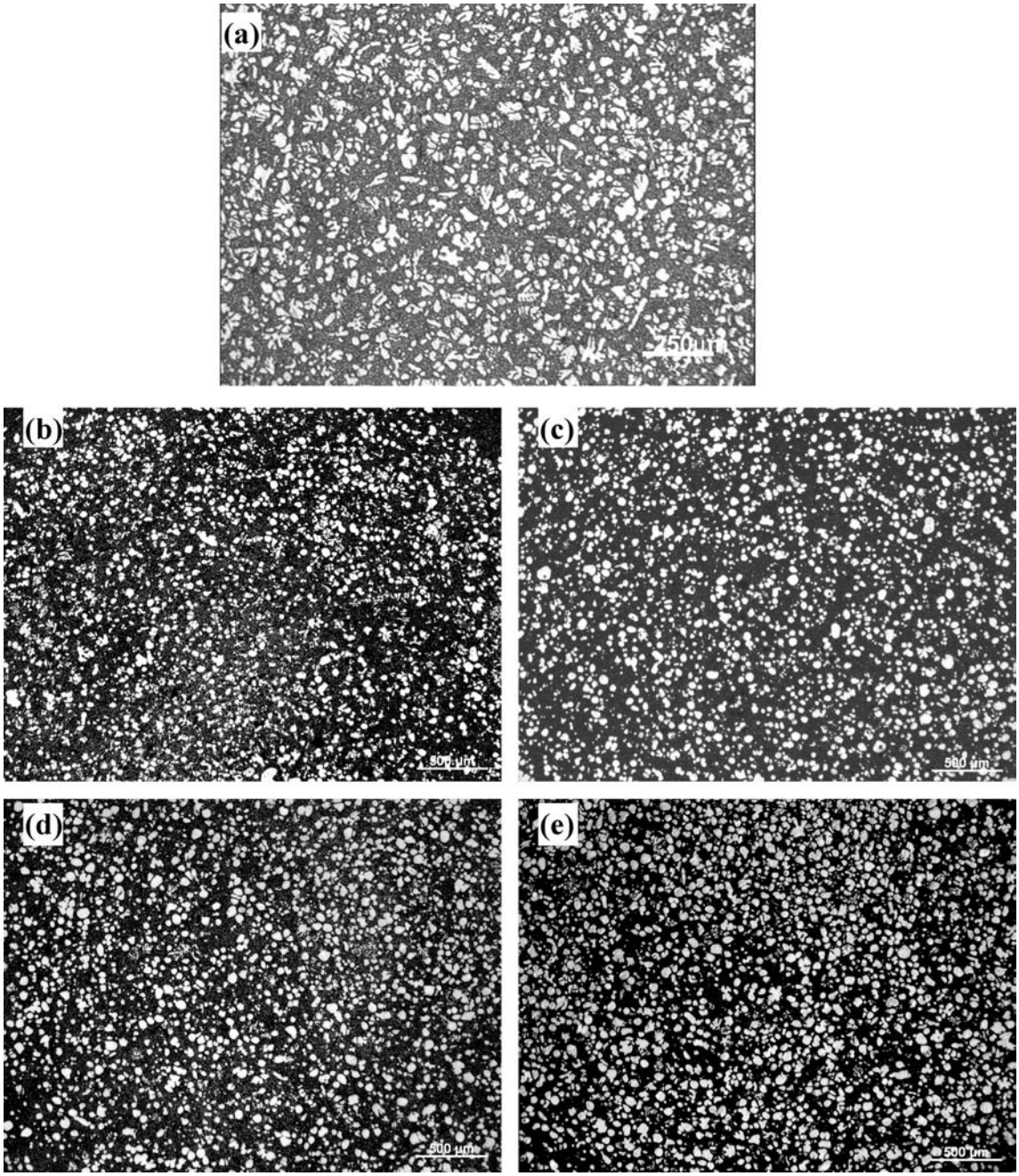

Figure 6 Micrographs of the microstructure for the RDC AZ91D alloy produced at, (a) 600°C (very close to melting temperature), (b) 597°C, (c) 593°C, (d) 589°C and (e) 585°C.

semisolid slurry inside the die cavity, without shearing, is referred to as secondary solidification. It is important to point out that the remaining liquid has been intensively sheared inside the slurry maker. Fig. 8 presents the microstructure produced by secondary solidification. The solidification of the remaining liquid produced further volume fraction of primary α-Mg particles (the dark area), with a fine size and a nearly spherical morphology, followed by the formation of a continuous eutectic network (the bright area). The particle size of the primary phase from the secondary solidification was quantified and presented, as a function of the processing temperature, in Fig. 9. It was found to be around 6 μm and independent of processing temperature. The detailed microstructure of the eutectic network is shown in Fig. 10a and b. It is interesting to see that the eutectic was completely divorced. The β-phase formed its own network and it was difficult to distinguish the eutectic α-phase and the primary α-phase produced by secondary solidification.

Fig. 10c and d present a SEM micrograph and the EDS line scan results, respectively, and show the compositional variation across a primary α-Mg particle. It can be seen that concentrations of Mg and Al inside the primary α-Mg particle were constant, and that a sharp increase in

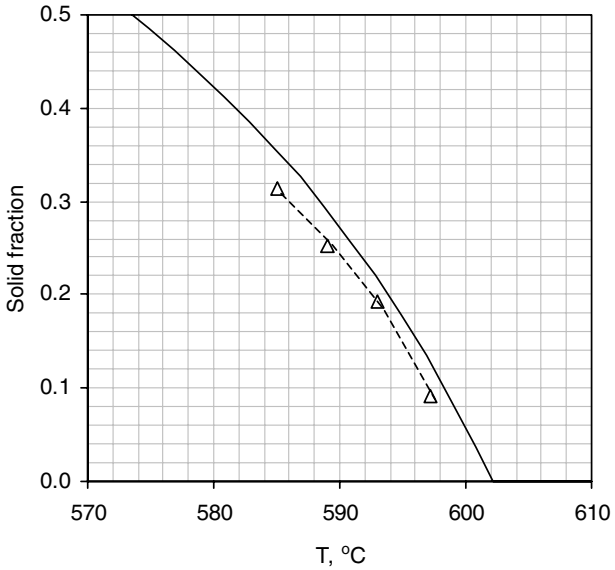

Figure 7 The calculated solid fraction of the AZ91D alloy as a function of temperature (the solid line) in comparison with experimental data (the triangles).

Al content was found when the probe was crossing the eutectic β-$Mg_{17}Al_{12}$ phase. This indicates local micro-segregation due to the coring effect. Czerwinstki *et al.* [19] detected an obvious increase in Al concentration when the electron probe beam moved from the centre towards the primary α-Mg particle boundary, indicating the coring effects. Dargusch and Dunlop [20] also found similar micro-segregation in their die-cast AZ91D alloy. Further EDS analysis of the chemical composition of the primary particles and the regions produced by secondary solidification gave the composition of the solid and liquid phases at the semisolid temperature (593°C), which are summarised in Table IV. The comparison between EDS analysis and thermodynamic prediction in Table IV indicates that the solidification process inside the twin-screw slurry maker was very close to equilibrium. However, the presence of the eutectic structure in Figs 8, 10a and b show that the secondary solidification was highly non-equilibrium. A vertical section of equilibrium phase diagram for ternary Mg-Al-Zn system at constant Zn content (0.67 wt%) were predicted by Thermo-Calc and MG-DATA (a Mg-database developed by Thermo-Tech Ltd, Guildford, UK), as shown in Fig. 11. Under equilibrium condition, AZ91D alloy should solidify as a single phase α-Mg solid solution, and further cooling should lead to the solid state precipitation of the $Mg_{17}Al_{12}$ β-phase. However, the solidification structure of Mg-Al alloys in the as cast condition differs significantly from this prediction. Non-equilibrium eutectic is always present in the as-cast microstructure in Mg-Al alloys containing more than about 2 wt.% Al [21]. Therefore, it can be concluded that in the RDC process the primary solidification under intensive forced convection is fairly close to equilibrium, while the secondary solidification inside the die without shearing is highly non-equilibrium.

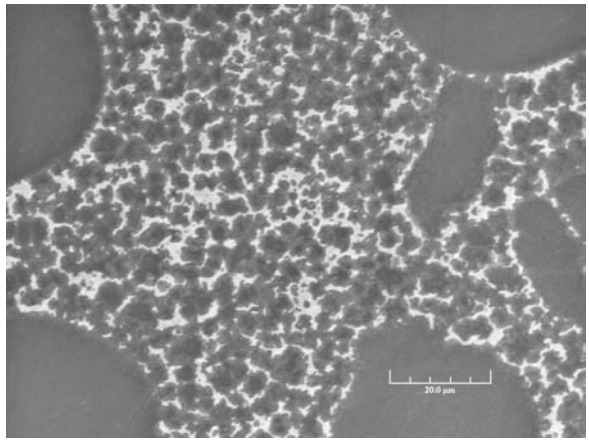

Figure 8 SEM back-scattered electron image showing the detailed microstructure of the RDC AZ91D alloy produced by secondary solidification inside the die cavity without shearing.

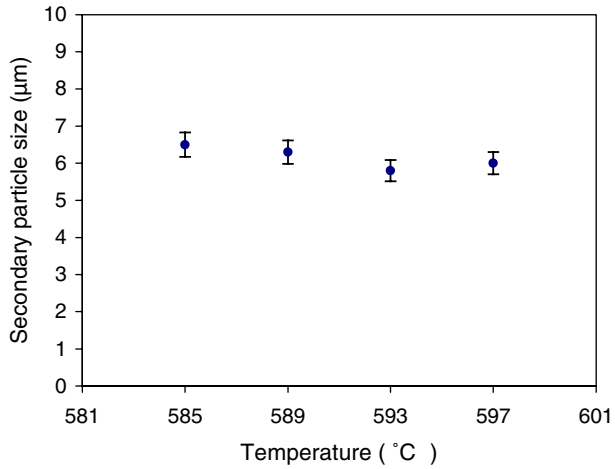

Figure 9 A graph to show the average size of the primary α-phase produced by the secondary solidification as a function of the processing temperature.

Oxide inclusions due to mixing with the dross and the inclusion of oxide skin of the ingots are always detrimental to the quality of castings produced by any casting process [22]. This detrimental effect is particularly severe for Mg casting. Mg has a high affinity to oxygen and any improper protection during melting and casting can cause excessive oxidation. In addition, the density of magnesium oxide is nearly twice as high as that of liquid Mg alloy. There is a continuous sedimentation of oxides from the dross layer to the melt. Detailed microstructural examination confirmed that, with appropriate protection, the RDC process does not increase the oxide content in the RDC samples. In order to examine the status of the oxide in the RDC samples, dross from the melting furnace was deliberately added to the Mg melt. Fig. 12 is a backscattered SEM micrograph showing the morphology of oxide particles in the RDC sample with added extra dross. The oxide particles, as identified by EDS analysis, are fine in size (less than 3 μm), spherical in morphology and uniform in distribution. No clusters of oxide particles and no evidence of any oxide skin were found in the

RDC samples, even with the added extra dross. This is attributed to the highly dispersive mixing power of the twin-screw slurry maker. Agglomerates of oxide particles and oxide film, if any, would be pulverised, spheroidised and dispersed by the intensive forced convection in the slurry maker.

4.3. Mechanical properties of RDC AZ91D alloy

The mechanical properties of RDC AZ91D alloy in the as-cast condition are presented in Table V, and compared to those of the same alloy produced by other processes in the literature [19, 23–25]. RDC samples showed improved ultimate tensile strength (UTS) to those obtained from both HPDC process and any other semisolid processing techniques. Perhaps more importantly, the RDC process offers a substantial increase in tensile elongation. This is significant because Mg-alloys, particularly AZ alloys, usually suffer from low ductility in the as-cast condition. The substantially improved ductility provided by the RDC process can promote wider applications of Mg-alloys.

Due to the extremely low or even eliminated porosity in RDC samples, heat treatment can be used to further enhance mechanical properties. The mechanical properties of RDC samples under different heat treatment conditions are tabulated in Table VI. Compared with the as-cast condition (RDC), T4 heat treatment improves ductility substantially but decreases strength. Both T6 and T5 reduce or maintain strength with some sacrifice of ductility.

4.4. Component production trials

Trials of component production have been conducted to confirm the reliability of the slurry maker and consistency of the RDC process. A component die was selected (the identity of the component is omitted here), which has two cavities and four sliding cores. The component die was originally designed for Al-alloys, and was used here for rheo-diecasting Mg component without any modification. A production trial was carried out in our laboratory using this component die. The section thickness of the component varied between 2 and 6 mm, the runner had a thickness of 10 mm and the biscuit was 60 mm in diameter. The trial results indicate that the RDC components have a very good surface finish, close to zero porosity and very fine and uniform microstructure throughout the entire casting, including the runners and biscuit. Fig. 13 presents a photograph of the casting with runners and biscuit and micrographs showing the microstructures at different positions in the casting. In contrast to the usual large variation of microstructure in HPDC samples, the RDC Mg samples had a constant microstructure, irrespective of the section thickness.

Fig. 14 shows the chemical composition of the RDC component (shown in Fig. 13) as a function of position. Position 1 is the biscuit, 2 is the runner and positions 3–6 are located at various parts of the component. In Fig. 14, Series A and Series B refer to two different components in one casting. Fig. 14 indicates that the chemical composition of the RDC sample was consistent throughout the entire casting, including the runner and biscuit. The Al content varied between 8.8 and 9.2 wt%, and Zn between 0.6 and 0.7 wt%.

TABLE IV Comparison between chemical compositions (wt.%) of the liquid and solid phases at 593°C obtained by SEM/EDS analysis and thermodynamic predictions

Alloying element		Mg	Al	Zn
Liquid	SEM/EDS	89.25 ± 0.22	9.66 ± 0.19	1.09 ± 0.03
	Thermo-Calc	89.82	10.35	0.83
Solid	SEM/EDS	97.17 ± 0.21	2.74 ± 0.20	0.093 ± 0.01
	Thermo-Calc	96.95	2.99	0.064

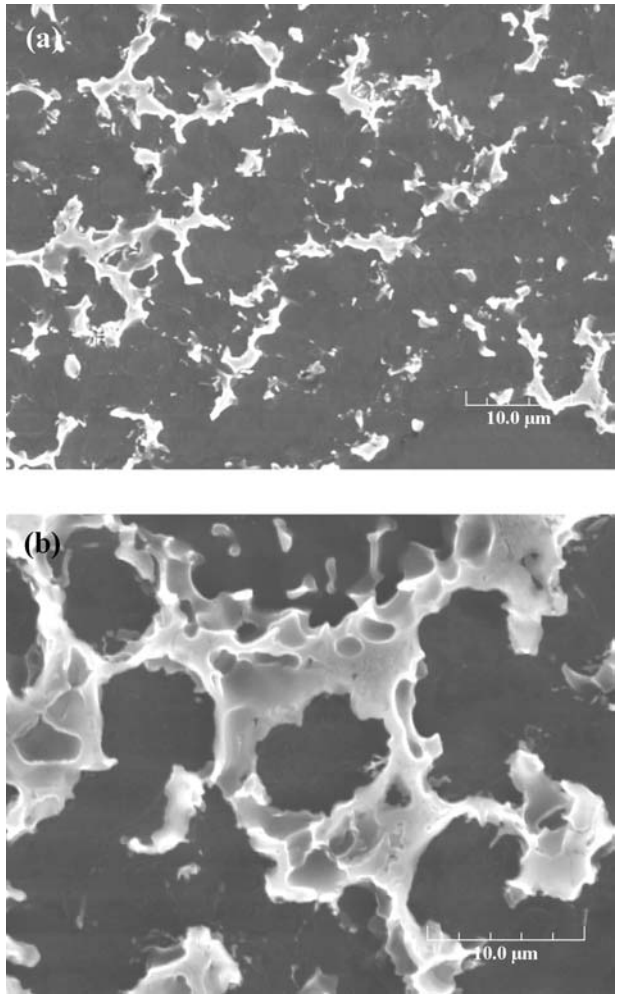

Figure 10 SEM micrographs of the RDC AZ91D alloy showing the detailed morphology of the β-$Mg_{17}Al_{12}$ phase formed through eutectic solidification. (a) At lower magnification showing the $Mg_{17}Al_{12}$ β-phase network, (b) at higher magnification showing the divorced nature of the metastable eutectic, (c) backscattered electron image and (d) EDS line scan results showing the compositional variation across a primary α-Mg particle.

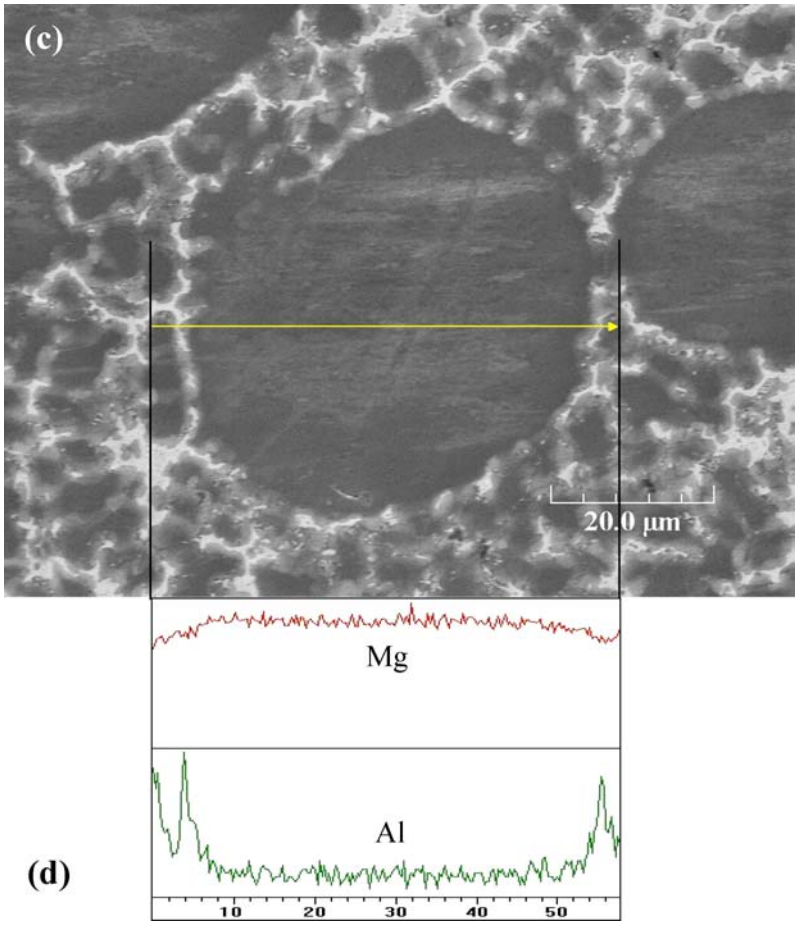

Figure 10 Continued.

5. Discussion

5.1. Rheological consideration of the RDC process

The most important objective of SSM processing is to achieve laminar die filling avoiding gas entrapment by increasing the viscosity of the feed material, while maintaining adequate fluidity for complete die filling. Intensive experimental investigations [4, 5, 10, 26] have confirmed the effects of the particle morphology on the flow behaviour of semisolid slurries. The morphological effects have been modelled successfully through effective solid fraction by Chen and Fan [27]. Both dendrites and rosettes entrap liquid inside individual particles resulting in an increased solid fraction, therefore decreasing the processability of the alloy. Another factor affecting the viscosity of a semisolid slurry is particle agglomeration. Particle agglomerates behave much like dendrites by entrapping liquid between particles, resulting in similar effects on processing. In addition, the currently used alloys for SSM processing usually have a small processing window due to the large temperature sensitivity of solid fraction in that 1 K variation in processing temperature can lead to a 5–10% change in solid fraction. Any negative effect on viscosity due to particle morphology and agglomeration can further reduce the processing window. Rheological understandings achieved through both experimental investigations and theoretical modelling allow one to have a clear target for process development, i.e., the ideal semisolid slurry for semisolid processing, which can be described as a suitable volume fraction of solid particles, with fine particle size and spherical morphology, dispersed uniformly throughout a liquid matrix. The ideal semisolid slurry can be achieved by controlling the nucleation and growth processes during solidification, as will be discussed further in the following section.

The experimental results presented previously show that the semisolid slurry provided by the twin-screw slurry maker has fine and spherical particles distributed uniformly in the liquid matrix. The positive effects of such high quality semisolid slurry on the die filling process have been confirmed by the experimental results presented in Fig. 4. A planar melt front can be achieved under the optimised processing conditions, resulting in the elimination of gas entrapment.

5.2. Solidification behaviour of AZ91D alloy

Solidification takes place in the RDC process in two distinct stages; the solidification inside the twin-screw slurry maker, under intensive forced convection, to produce semisolid slurry is referred to as primary solidification,

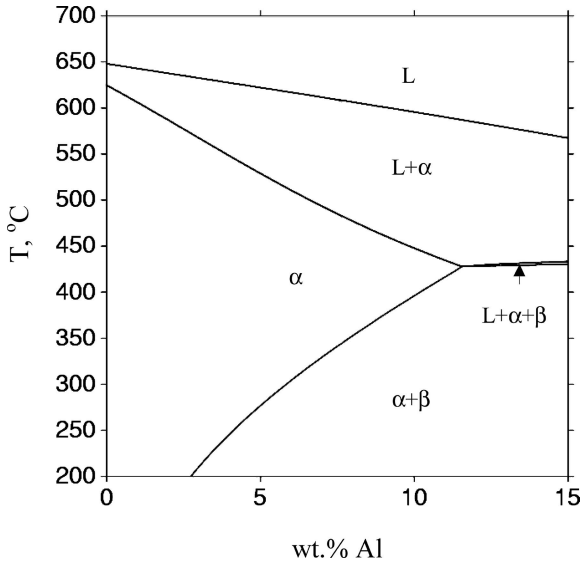

Figure 11 A vertical section of the Mg-Al-Zn ternary equilibrium phase diagram with the Zn content being fixed at 0.67 wt.%.

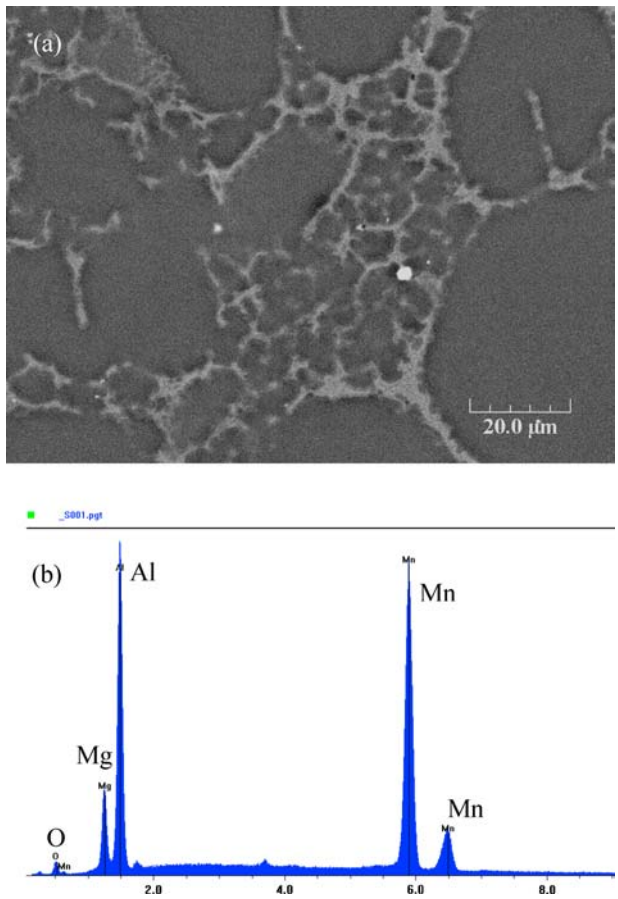

Figure 12 (a) SEM back-scattered electron image and (b) the corresponding EDS spectrum showing the morphology of the dispersed oxide particles, in an as-cast AZ91D alloy with added extra dross.

while the solidification of the remaining liquid inside the die cavity, without shearing, is referred to as secondary solidification. This two-stage solidification process is discussed here in terms of nucleation and growth.

In the conventional casting processes, overheated liquid metal is poured into the relatively cold mould. Heterogeneous nucleation takes place immediately in the undercooled liquid close to the mould wall. The majority of the nuclei are transferred to the overheated liquid region and dissolved, so only a small proportion (as low as 0.3% [28]) of the nuclei survive and contribute to the final microstructure, giving rise to a coarse and non-uniform microstructure. It is clear that an important step towards microstructural refinement is to make sure that every single nucleus formed during nucleation can survive and contribute to the final microstructure. Through both theoretical and experimental studies, the following conditions have been identified to achieve 100% nucleus survival rate: (1) uniform temperature and chemical composition throughout the entire volume of the liquid alloy during the continuous cooling process; (2) well-dispersed heterogeneous nucleation agents. Under such conditions, nucleation will occur throughout the entire volume of the liquid and each nucleus will survive and contribute to the final solidified microstructure, producing a fine and uniform microstructure. We refer to nucleation under such conditions as 'effective nucleation'. The next step towards the ideal semisolid slurry is to ensure the nuclei that survive grow into spherical particles rather than dendrites or rosettes. Our theoretical analysis on morphological evolution during solidification [29] has revealed that, with increasing shear rate and the intensity of turbulence, the growth morphology changes from dendrites to spheres via rosettes, due to the change in the diffusion geometry in the liquid around the growing solid phase. This theoretical prediction of the morphological change from dendritic growth to spherical growth with increasing shear rate and intensity of turbulence has been verified experimentally [30]. To sum up, the conditions to achieve spherical crystal growth are high shear rate and high intensity of turbulence.

The conditions to ensure effective nucleation and spherical growth can be achieved through the twin-screw mechanism. The fluid flow inside the twin-screw device is characterised by high shear and high intensity of turbulence. The shear dispersive mixing power of the twin-screw device ensures the uniformity of both temperature and chemical composition during the continuous cooling process. In addition, there is a large and ever-renewing interfacial area between the cooling melt, the screws and barrel. This is ideal for enhancing the efficiency of heat exchange during solidification, resulting in a highly efficient slurry making process. For a given charge to the slurry maker, the slurry maker can transform the liquid Mg-alloy into SSM slurry within 20–30 s. Furthermore, such enhanced kinetic conditions during the primary solidification would give rise to equilibrium or close to equilibrium solidification, as supported by the experimental results presented previously.

TABLE V Mechanical properties of the RDC AZ91D alloy in comparison with those of the same alloy produced by different processing technologies

Process	Yield strength (MPa)	UTS (MPa)	Elongation (%)	Reference
HPDC	146	212	3.3	[23]
Thixocasting	134	223	3.6	[24]
Thixomoulding	–	150–241	3–5	[20]
New rheocasting (NRC)	–	230	5.5	[25]
Rheo-diecasting (RDC)	145	248	7.4	This work

TABLE VI Mechanical properties of RDC AZ91D alloy under different heat treatment conditions

Heat Treatment	Conditions	Yield strength (MPa)	UTS (MPa)	Elongation (%)
RDC	As-cast	145	248	7.4
RDC + T4	413°C, 5 h	91	230	11.2
RDC + T5	216°C, 5 h	133	236	6.5
RDC + T6	413°C, 5 h + 216°C, 5.5 h	134	255	6.7

Unlike primary solidification under intensive forced convection, secondary solidification is characterised by high cooling rate without shearing. Although the remaining liquid in the SSM slurry will solidify in the die cavity without shearing, it has been intensively sheared in the twin-screw slurry maker. It therefore has a uniform temperature and composition throughout the liquid. According to the previous analysis, nucleation would occur throughout the entire remaining liquid, and every single nucleus would survive, contributing to the final microstructure. However, in contrast to the nucleation in the twin-screw slurry maker, nucleation in the die cavity will occur with a much higher nucleation rate due to the high cooling rate provided by the metallic die (in the order of 10^3 K/s) of the HPDC machine. Under such conditions, each nucleus would not have much chance to grow before the remaining liquid is completely consumed, resulting in a very fine structure (Figs 8 and 9). Another consequence of the high cooling rate is the departure from equilibrium solidification, resulting in the formation of a substantial amount of non-equilibrium eutectic structure (Fig. 10), which is not predicted by the equilibrium phase diagram in Fig. 11.

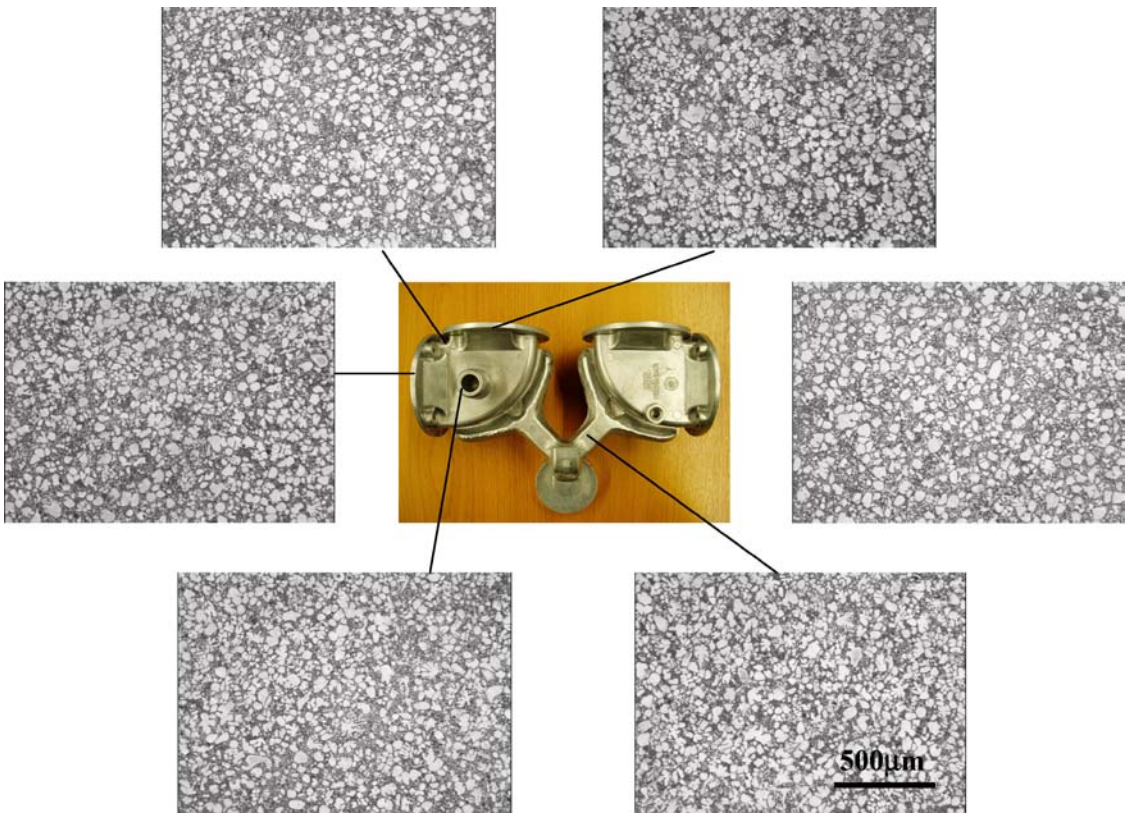

Figure 13 Optical micrographs showing the microstructure of the RDC AZ91D alloy component at different locations. All the micrographs have the same magnification.

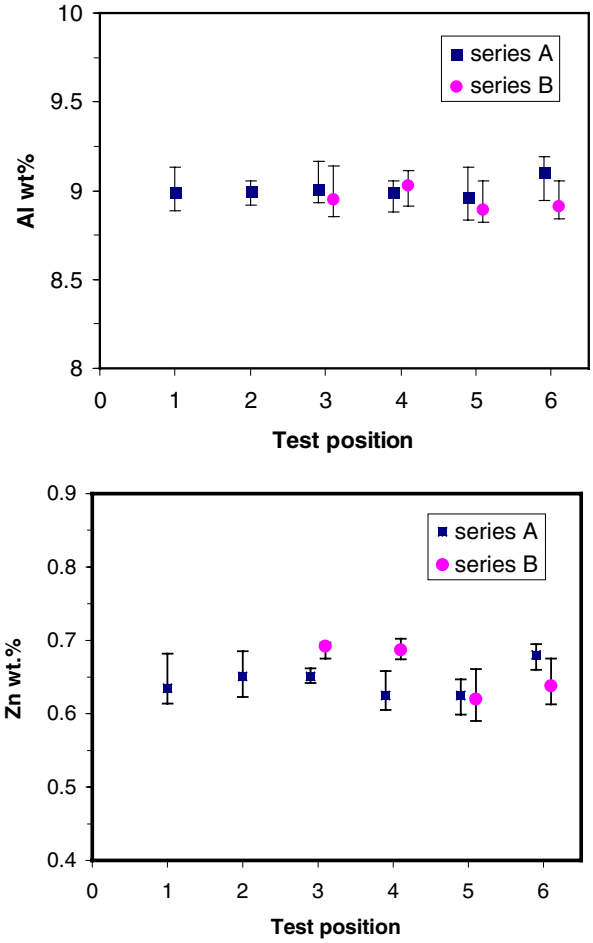

Figure 14 The chemical compositions of a RDC AZ91D alloy casting (shown in Fig. 13) as a function of location showing the chemical uniformity. Position 1 is the biscuit, position 2 is in the runner and positions 3–6 are located at various parts of the component. Series A and Series B refer to two different components in one casting.

5.3. Mechanical properties of RDC AZ91D alloy

Mechanical testing, along with microstructural characterisation, was used to optimise the RDC process for AZ91D alloy. The yield strength of the Mg alloy has a strong dependence on grain size [31]. For the RDC samples the microstructure is fairly constant in terms of grain structure. It is reasonable to expect a fairly constant yield strength at the level given in Table V. However, the UTS is largely determined by the amount of defects present in the sample. The major defects affecting UTS are gas pores, hot cracks and microstructural non-uniformity [32]. The larger the amount of defects, the lower the UTS and the elongation. Under the optimised condition, the RDC samples have very little or are free from porosity, and have a uniform microstructure. This in turn will lead to higher strength and elongation compared with samples obtained by other processing techniques, as shown by the comparison in Table V.

In the RDC microstructure, the divorced eutectic β-phase forms a continuous network (Fig. 10). The β-phase is a brittle intermetallic compound. Such network would be harmful to ductility. Under T4 condition, the RDC structure transforms into a single α-phase structure through solid solutioning, eliminating the brittle β-phase network. Consequently an increased elongation is expected, as confirmed by the experimental results presented in Table VI. Ageing of the RDC samples produces coarse laminar $Mg_{17}Al_{12}$ precipitates, through initially discontinuous precipitation at grain boundaries and then continuous precipitation in the grain interior [14]. Due to the incoherent nature of the β-precipitates in the α-Mg phase, the precipitation strengthening effect is rather weak. This explains why (compared to the T4 condition) only a moderate increase in strength of the RDC samples can be achieved by heat treatment under both T5 and T6 conditions. It seems that for AZ91D alloy the only effective heat treatment is T4 for improving the ductility of the cast samples and that both T5 and T6 does not improve the tensile mechanical properties under the present experimental conditions.

5.4. Advantages of the rheo-diecasting process

Based on our experiments for process optimisation and component production trials, we have identified the following advantages of the RDC process over the conventional HPDC process:

- A fine and uniform microstructure resulting from enhanced effective nucleation and spherical growth during solidification under high shear rate and high intensity of turbulence.
- Close-to-zero porosity (well below 0.5 vol.%), due to the elimination of the entrapped air by laminar mould filling and much reduced hot tearing, due to the lower die filling temperature.
- RDC components can be subjected to full heat treatment for enhancing mechanical performance, without compromising the surface quality and dimensional control.
- Well-dispersed oxide particles with fine size and spherical morphology, achieved by the dispersive mixing power of the twin-screw mechanism.
- The extensively sheared liquid in the semisolid slurry solidifies in the die cavity producing very fine α-phase and a divorced eutectic structure, which are favourable to the property enhancement.
- Improved mechanical properties, particularly elongation, due to the structural refinement and uniformity, reduced or even eliminated porosity and other cast defects.
- Suitable for components with varying section thickness
- Lower scrap rate and a higher material yield.
- Lower overall component production cost due to higher productivity, lower scrap rate and a higher material yield.

- The RDC process can be achieved by simply attaching the slurry maker to a cold chamber HPDC machine.

6. Conclusions

1. A new semisolid metal processing technology, rheo-diecasting (RDC), has been developed for the production of Mg-alloy components with high integrity. Rheo-diecasting can be readily achieved by adding a twin-screw slurry maker to an existing cold chamber die-casting machine.

2. Solidification in the RDC process takes place in two distinct stages; one is primary solidification in the twin-screw slurry maker, which is close to equilibrium and the other one is secondary solidification in the die cavity, which is highly non-equilibrium.

3. The fluid flow inside the twin-screw slurry maker is characterised by high shear rate and high intensity of turbulence, which in turn promote effective nucleation and spherical growth during primary solidification, resulting in a fine and uniform microstructure.

4. Secondary solidification takes place uniformly throughout the entire die cavity producing an extremely fine and uniform microstructure.

5. Under optimised conditions the rheo-diecast samples have close-to-zero porosity and a fine and uniform microstructure throughout the entire component, without any chemical segregation.

6. The RDC process provides components with improved ultimate tensile strength and ductility in the as-cast condition compared with HPDC or other available semisolid processing techniques.

7. Heat treatment can be used to enhance the mechanical properties of RDC samples. For RDC AZ91D Mg alloy, T4 heat treatment significantly improves ductility but with substantial decrease in strength, while both T5 and T6 improve strength moderately but decrease the ductility, compared with the T4 condition.

Acknowledgments

The authors acknowledge the contribution to this work from Drs S. Ji, Y. Liu, E. Zhang and Z. Zhen. Financial support from EPSRC (UK), Ford Motor Co and Magnesium Elektron Ltd. (UK) is also acknowledged with gratitude.

References

1. H. FRIEDRICH and S. SCHUMANN, in Proceedings of the 2nd Israeli International Conference of Mg Science and Technology, (Dead Sea, Israel, 2000) p. 9.
2. A. BALASUNDARAM and A. M. OKHALE, in "Magnesium Technology 2001," edited by J. Hryn (TMS, 2001) p. 155.
3. H. FRIEDRICH and S. SCHUMANN, in Proceedings of IMA 2001 Magnesium Conference (Brussels, Belgium, 2001) p. 8.
4. M. C. FLEMINGS, *Metall. Trans.* **22A** (1991) 957.
5. D. H. KIRKWOOD, *Inter. Mat. Rev.* **39** (1994) 173.
6. K. P. YOUNG, US Patent, No. 4,687,042, 1987.
7. ALUMAX Inc., European Patent Specifications, EP 0 071 822 B2, 1982.
8. M. P. KENNEY, J. A. COURTOIS, R. D. EVANS, G. M. FARRIIOR, C. P. KYONKA, A. A. KOCH and K. P. YOUNG, in "Metals Handbook," 9th edition (Metals Park, OH, ASM International) Vol. 15, pp. 327.
9. L. PASTERNAK, R. D. CARNAHA, R. DECKER and R. KILBERT, in Proc. the 2nd International Conference on Semi-Solid Processing of Alloys and Composites, edited by S. B. Brown and M. C. Flemings (MIT, Cambridge, 1992) p. 159.
10. Z. FAN, *Inter. Mater. Rev.* **47** (2002) 49.
11. H. KAUFMANN, H. WABUSSEG and P. J. UGGOWITZER, *Aluminium* **76** (2000) 69.
12. J. A. YURKO, R. A. MARTINEZ and M. C. FLEMINGS, in: Proceedings of the 7th International Conference on Semisolid Metal Processing, edited by Y. Tsutsui, M. Kiuchi and K. Ichikawa, Tsukuba, Japan (2002) p. 659.
13. M. FINDON, A. M. DE FIGUEREDO, D. APELIAN and M. MAKHLOUF, in Proceedings of the 7th International Conference on Semisolid Metal Processing, edited by Y. Tsutsui, M. Kiuchi and K. Ichikawa, Tsukuba, Japan (2002) p. 557.
14. Y. WANG, G. LIU and Z. FAN, *Acta Mater.*, **54** (2006) 689.
15. Magnesium and Magnesium Alloys, ASM Speciality Handbook (ASM International, The Materials Information Society, 1999).
16. W.P. SEQUEIRA, G. L. DUNLOP and M. T. MURRAY, in Proceedings of the 3rd International Mg Conference, edited by C. Baker, R.L. Edgar, H. Jones and J. F. King (London, (Institute of Materials, 1996) p. 63.
17. A. L. BOWLES, J. R. GRIFFITHS and C. J. DAVIDSON, in "Magnesium Technology 2001," edited by J. Hryn (TMS, 2001) p. 161.
18. Z. FAN and S. JI, UK patent application No. 0019856.4, 11th August 2000.
19. F. CZERWINSKI, A. ZIELINSKA-LIPIEC, P. J. PINET and J. OVERBEEKE, *Acta Mater.* **49** (2001) 1225.
20. M. S. DARGUSCH and G. L. DUNLOP, in "Magnesium Alloys and their Applications," edited by B. L. Mordike and K. U. Kainer (Wolfsburg, Germany, 1998) p. 277.
21. I. J. POLMEAR, in "Light Alloys, Metallurgy of the Light Metals," 3rd ed. (Butterworth Heinemann, 1995).
22. G. G. WANG, B. FROESE and P. BAKKE, in "Magnesium Technology 2003," edited by H. I. Kaplan (TMS, 2003) p. 65.
23. C. PITSARIS, T. ABBOTT, C. H. J. DAVIES and G. SAVAGE, in "Magnesium," edited by K.U. Kainer, Proceedings of the 6th International Conference of Magnesium Alloys and Their Applications", Weinheim (Wiley-VCH, Verlay GmbH & Co. KGaA, 2003) p. 694.
24. J. AGUILAR, T. GRIMMING and A. BÜHRIG-POLACZEK, in "Magnesium, Proceedings of the 6th International Conference of Magnesium Alloys and Their Applications", edited by K. U. Kainer, Weinheim (Wiley-VCH, Verlay GmbH & Co. KGaA, 2003) p. 767.
25. H. KAUFMANN and P. J. UGGOWITZER, in "Magnesium Alloys and Their Applications," edited by K. U. Kainer (Wiley-VCH, Verlay GmbH & Co. KGaA, 2000) p. 533.
26. P. A. JOLY and R. MEHRABIAN, *J. Mater. Sci.* **11** (1976) 1393.
27. J. Y. CHEN and Z. FAN, *Mater. Sci. Tech.* **18** (2002), 237, 243, 250, 258.
28. P. D. LEE, Private Communication, Department of Materials, Imperial College, London, 2003.
29. A. DAS, S. JI and Z. FAN, *Acta. Mater.* **50** (2002) 4571.
30. S. JI and Z. FAN, *Met. Mater. Trans.* **33A** (2002) 3511.
31. P. ANDERSSON, C. H. CASERES and J. JOIKE, *Mater. Sci. Forum* **419–422** (2003) 123.
32. A.M. GOKHALE and G. R. PATEL, in "Magnesium Technology 2001," edited by J. Hryn (TMS, 2001) p. 195.

Received 25 May
and accepted 15 August 2005